Hindawi
Journal of Nanoscience
Volume 2017, Article ID 2409062, 9 pages
https://doi.org/10.1155/2017/2409062

Research Article

Spreadability of Ag Layer on Oxides and High Performance of AZO/Ag/AZO Sandwiched Transparent Conductive Film

Yuchao Niu,[1,2] Xiaoyu Ma,[1] Xiangju Liu,[2] Weimin Wang,[3] Yongtai Zhen,[4] and Ying Gao[2]

[1] *Co-Innovation Center for Green Building, Shandong Jianzhu University, Jinan 250101, China*
[2] *School of Materiel Science and Engineering, Shandong Jianzhu University, Jinan 250101, China*
[3] *The Key Laboratory for Liquid-Solid Structural Evolution & Processing of Materials, Ministry Education, Shandong University, Jinan 250061, China*
[4] *Shandong Yucheng Hanneng Solar Power Co., Ltd, Shandong, Yucheng 251200, China*

Correspondence should be addressed to Weimin Wang; weiminw@sdu.edu.cn

Received 3 April 2017; Accepted 12 June 2017; Published 25 July 2017

Academic Editor: Zhengjun Zhang

Single layers of indium tin oxide (ITO), aluminum-doped zinc oxide (AZO), and Ag, bilayers of ITO/Ag and AZO/Ag, and sandwiched layers of ITO/Ag/ITO (IAI) and AZO/Ag/AZO (ZAZ) were fabricated on ordinary glass substrates using magnetron sputtering. The surface morphologies of single layers and bilayers were measured. The sheet resistance and transmittance of the sandwiched layers were investigated. The results showed that the spreadability of the Ag on the AZO was significantly better than that on the ITO or bare glass substrate. The spreadability of Ag on underlayers influences obviously the performance of transparent conductive oxide/Ag/transparent conductive oxides (TCO/Ag/TCO or TAT). The sheet resistance and transmittance of the ZAZ sandwiched layer with the matching of 35 nm AZO (35 nm)/Ag (9 nm)/AZO (35 nm) fabricated in this paper were low to 3.84 Ω/sq and up to 85.55% at 550 nm, respectively. Its maximum Haacke figure of merit was 0.05469 Ω^{-1}, higher than that of IAI multilayer.

1. Introduction

Indium tin oxide (ITO)/metal/ITO (IMI), aluminum-doped zinc oxide (AZO)/metal/AZO (ZMZ), fluorine-doped tin oxide (FTO)/metal/FTO (FMF), and so forth as the most popular transparent conductive oxides (TCO)/metal/transparent conductive oxide TCO (TMT) have been widely studied [1–13]. Because the transparent conductive properties of TMT depended mainly on the metal layer [1, 9, 14–16], a variety of researches on TMT focused on the metal layer [2, 17–22]. Generally, the thickness of metal layer was about 8–14 nm [1] because the too thick metal layer made the light transmittance decrease while the too thin one did not form a continuous layer and made the electrical conductivity decrease dramatically. From this point of view, for a thinner metal layer to form a continuous one is a very important issue.

Recently, the thickness of a continuous Cu layer in ZnO/Cu(O)/ZnO sandwiched layer was only 5 nm. Its sheet resistance was as low as 9–13 $\Omega \cdot sq^{-1}$ and average transmittance over the visible spectral range of 400–800 nm was 83–85% with a maximum transmittance of 94% [20]. Compared with Cu layer, the Ag layer had a much lower sheet resistance, a higher transmittance, and lower absorption at the same thickness in the visible region [23], so investigating the Ag layer growth during its initial stage is quite necessary since the continuity of a thin metal layer depends mainly on its growth behavior. The growth of Ag layer during its initial stage is affected by many factors, like substrate material kind, substrate surface topography, substrate temperature, deposition rate, deposition gas pressure, and so on. Among them, the substrates are undoubtedly important factors because they are related directly to the interaction of Ag atom with that of the substrate [24] and the nucleation and grain growth behavior of Ag layer [25–28]. In an earlier report [19], it was found that the spreading of Ag on the surface of ZnO was better than that on SnO_2 due to a better affinity between Ag and ZnO though surface of ZnO was rougher than that of the latter. It brings about a question whether there exists any difference between the spreading of Ag on the surface of ZnO and that on ITO. As far as we know, there are few

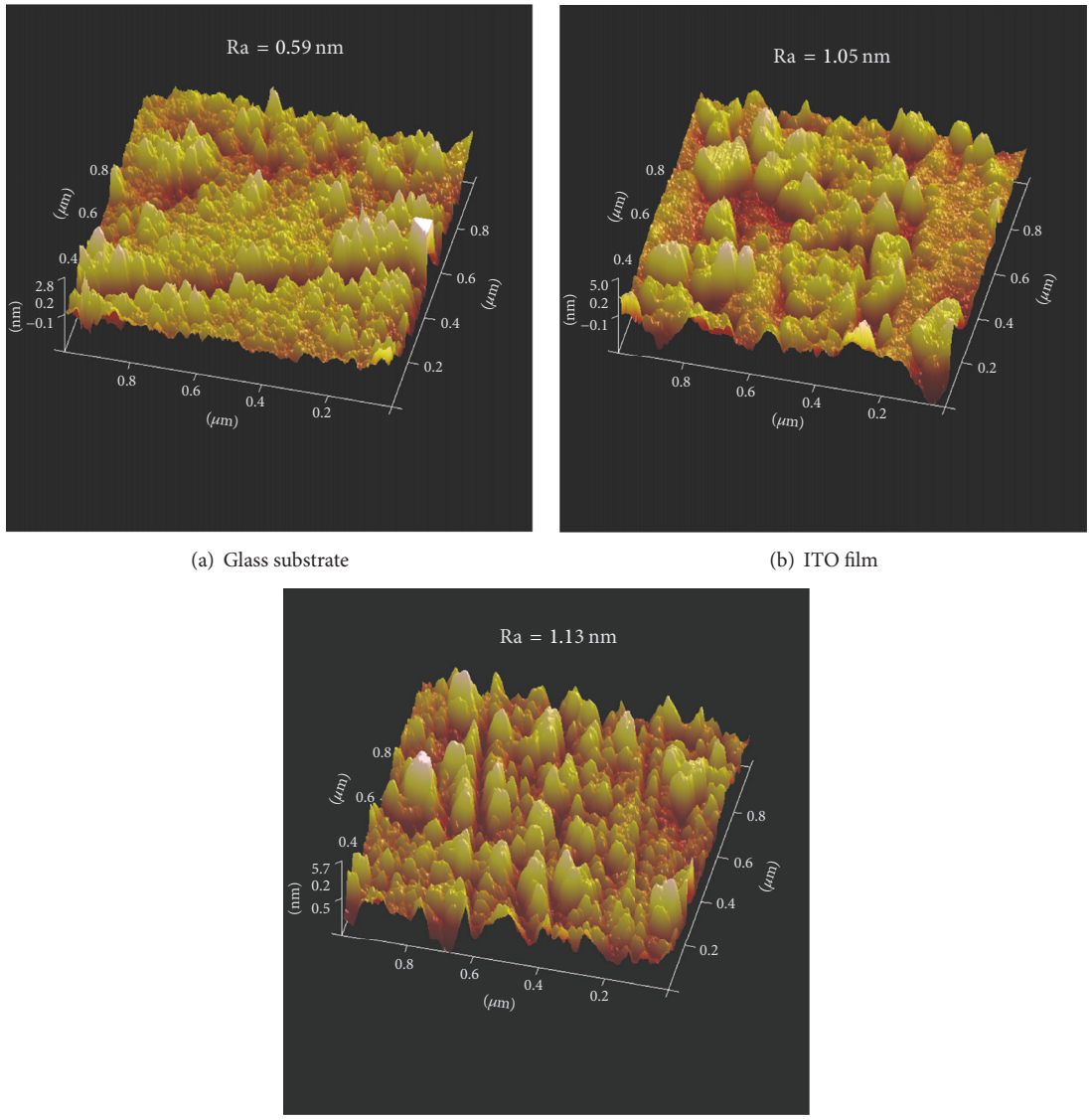

(a) Glass substrate

(b) ITO film

(c) AZO film

Figure 1: AFM morphologies of glass substrates, ITO, and AZO layers.

reports about the comparison between Ag initial growth and spreading on ITO and those on AZO.

In this paper, IAI and ZAZ were fabricated and the growth of Ag layer on ITO and that on AZO were compared. The effects of substrates on the microstructure and electrical property of Ag layer were investigated.

2. Experimental

Single layers of indium tin oxide (ITO), aluminum-doped zinc oxide (AZO), and Ag, bilayers of ITO/Ag and AZO/Ag, and sandwiched layers of ITO/Ag/ITO (IAI) and AZO/Ag/AZO (ZAZ) were fabricated, respectively, onto ordinary soda lime glass substrates (40 mm × 40 mm × 2 mm) using three-target sputtering. During the sputtering, the substrates were not heated or cooled. The targets of ITO (10% SnO_2, 90% In_2O_3), AZO (3% Al_2O_3, 97% ZnO), and Ag were all 60 mm in diameter. The distance between targets and substrates were 80 mm. The substrates revolved at 10 r/min. The sputtering chamber was first pumped to 6×10^{-4} Pa; then Ar gas was introduced to 1×10^{-1} Pa. The sputtering voltage and current for ITO target and AZO target were 420 V and 0.2 A, while those for Ag target were 360 V and 0.1 A.

An atomic force microscopy (AFM, Multimode-3D), a surface contourgraph (Alpha-Step IQ), a four-point probe resistivity measurement instrument (SB100A/20), a scanning electron microscopy (SEM, Supra 55), and a visible light photometric meter (723PCS) were used, respectively, to measure the surface profile, thickness, sheet resistance, surface morphology, and transmittance of the layers. In order to

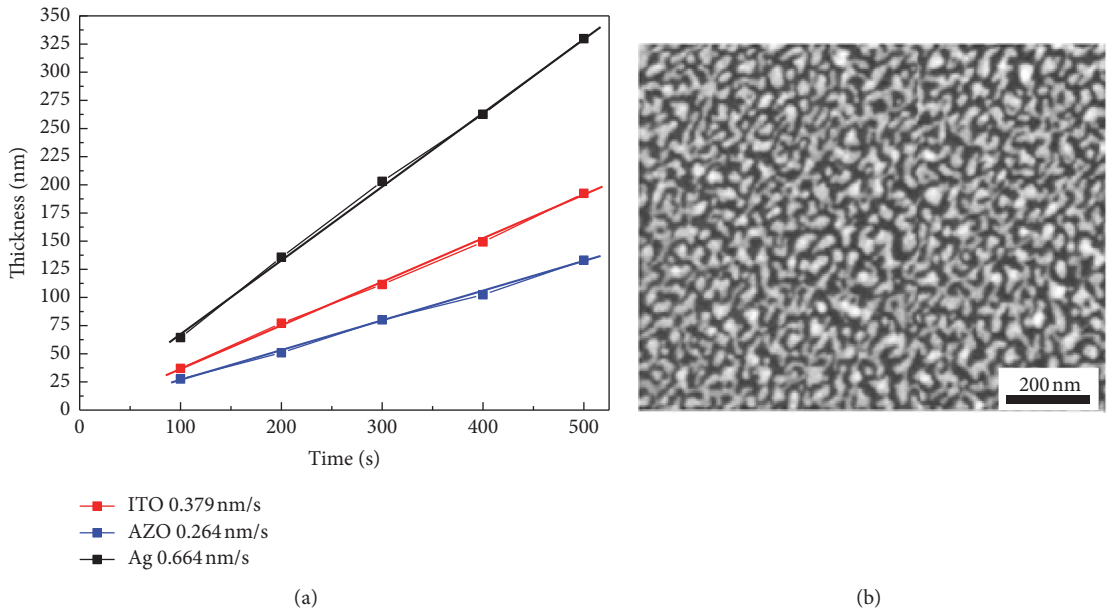

FIGURE 2: Average deposition rate of ITO and AZO (a) and Ag layer and the morphology of Ag layers (thickness of 4 nm) on glass substrate (b).

evaluate the overall merit of the layer, the Haacke figure of merit was used. Haacke figure of merit Φ_{TC} calculation formula is [29, 30]

$$\Phi_{TC} = \frac{T^{10}}{R_S}, \quad (1)$$

where T is the transmittance at 550 nm and R_S is the sheet resistance.

3. Results and Discussion

3.1. Spreadability of Ag on Underlayers. The AFM morphologies of the glass substrate and indium tin oxide (ITO) and aluminum-doped zinc oxide (AZO) underlayers deposited on the glass substrate with thickness of 25 nm are shown in Figure 1. The surface of glass substrate is smooth and its roughness is 0.59 nm. The surface roughness values of ITO layer and AZO layer are 1.05 and 1.13 nm, respectively, which are higher than those of the glass substrate.

In order to get the deposition rate of layers, the thick layers were deposited deliberately to ensure the measuring accuracy of the layer thickness. Figure 2(a) shows the relationship between thickness and deposition time of ITO, AZO, and Ag layers, respectively. Figure 2(b) shows SEM morphology of the Ag layers of 4 nm thickness on the glass substrate. It can be seen that the layer thickness is proportional to deposition time (Figure 2(a)). Therefore, the average deposition rates of the ITO, AZO, and Ag layers are 0.379 nm/s, 0.261 nm/s, and 0.664 nm/s, respectively. Hereafter, all layer thicknesses in this paper are deduced according to the deposition rates and times. It can be seen from the SEM picture that the islands on the glass have a big size and a bad spreadability (Figure 2(b)).

Figure 3 shows the surface morphology of the Ag layers with different thicknesses on the ITO and AZO layers, which were deposited on the glass substrate with the same thickness of 25 nm. In case of 4 nm Ag layer, since the time of deposition was short, the deposited Ag was too little to well cover the underlayers. Both Ag layers on the ITO and AZO underlayers appear in island shape. The voids between the islands on the AZO have the smaller size than those on the ITO, indicating Ag has a better spreadability on the AZO (Figures 3(a) and 3(e)). When the thickness of the Ag layer is 5 nm, there appear more connections between the Ag islands. The Ag layer on the AZO changes into a continuous structure, but that on the ITO does not (Figures 3(b) and 3(f)). When the Ag layer thickness increases to 6 nm the connections become stronger and the quantity of voids reduces. The Ag layer on the ITO changes into a continuous structure. The void fraction of the Ag layer on the AZO is much lower than that on the ITO (Figures 3(c) and 3(g)). When the thickness of Ag layer is up to 8 nm the void fraction reduces further and the size of voids also reduces remarkably. The Ag layers exhibit a continuous structure and most of the surface of the ITO and AZO layers is covered by Ag (Figures 3(d) and 3(h)). This layer growth order of island-net-layer is consistent with the mode of metal film growth [31]. Compared with that on the ITO layer, the morphology of Ag layer on the AZO layer is fine and the spreadability of Ag is better.

Figure 4 illustrates the relation between the sheet resistance and thickness of the Ag layers deposited, respectively on a bare glass substrate, the AZO, and ITO underlayers. These sheet resistance values are listed in Table 1. When Ag layer thickness is less than 4 nm, Ag layer has the island structure and the electrical connection is very poor, so that three samples with Ag layer have a bigger sheet resistance. With increasing the thickness, the Ag layer changes gradually from discontinuous structure to continuous structure (Figure 3), the sheet resistances of the samples with Ag layer decrease drastically.

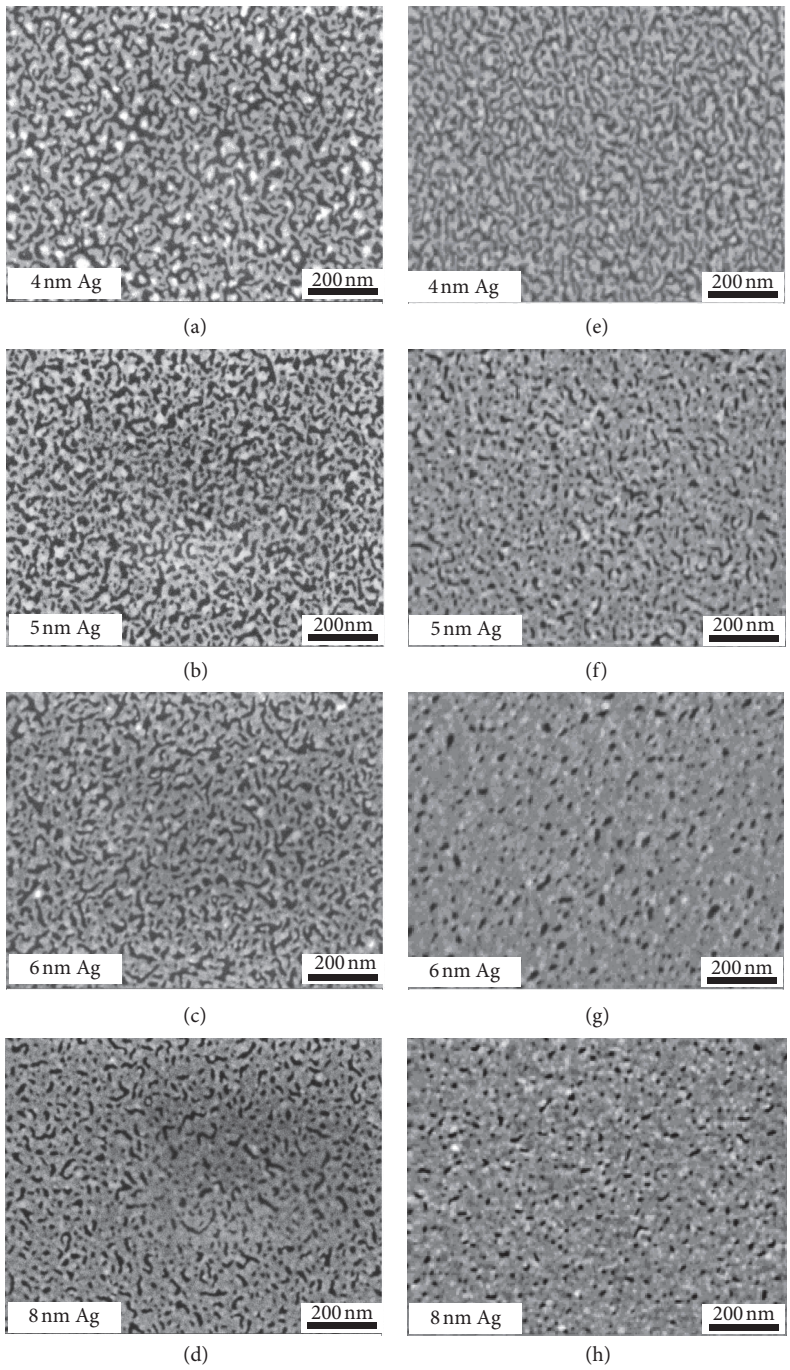

Figure 3: SEM morphologies of Ag layer with different thicknesses on the 25 nm underlayer: (a–d) on ITO, (e–h) on AZO.

However, when the thickness of Ag layer is beyond 8 nm the sheet resistance of the layer decreases slowly. With increasing the thickness of Ag layer, the sheet resistance of the Ag/AZO bilayer reduces and is even lower than that of the Ag/ITO bilayer. The reason may be related to the spreadability [19, 24] of the Ag layer on the AZO underlayer. As shown in Figure 3, the Ag layer deposited on the AZO has a better spreadability. As such, the connection between the Ag island structures on the AZO is better than that on the glass or ITO with the same deposition time. Therefore, it is understood that the sheet resistance of the Ag/AZO bilayer with Ag layer thickness ≥6 nm is lower than Ag/ITO counterparts (Table 1). In addition, since the conductivity of the ITO is superior to that of the AZO, the total conductivity of Ag/ITO bilayers with Ag layer thickness ≤4 nm is higher than that of Ag/AZO counterparts because Ag is in an island structure and the total conductivity is affected obviously by the underlayer. Therefore, the spreadability of the Ag layer with its underlayer plays an important role during the fabrication of a high performance TCO/Ag/TCO.

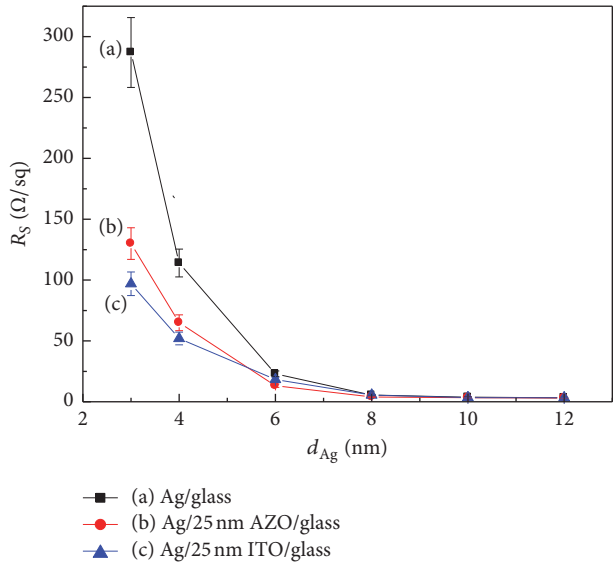

Figure 4: Relationship between sheet resistance and the thickness of Ag layer on different substrates.

Table 1: Sheet resistance related to thickness of the Ag layers.

Ag thickness, nm	R_S, Ω/sq		
	Ag/25 nm ITO/glass	Ag/25 nm AZO/glass	Ag/glass
0	625	17200	∞
3	97	130	287
4	52	65	114
6	18.3	13.2	23
8	5.53	4.02	5.53
10	3.45	3.34	3.75
12	3.28	3.11	3.31

3.2. The Performance of ZAZ Transparent Conductive Film. IAI and ZAZ sandwiched layers with different thicknesses were fabricated on ordinary glass substrates. The performances of these sandwiched layers are shown in Figure 5. The annotations below the curves are the ITO or AZO layer thickness (nm)/Ag layer thickness (nm)/ITO or AZO layer thickness (nm), and the sheet resistance ($\Omega \cdot sq^{-1}$) in turn. From the annotations inserted in the figures, the sheet resistance of the IAI and ZAZ sandwiched layers reduces obviously with increasing the thickness of Ag layer from 7 nm to 13 nm. However, the sheet resistance of the ZAZ is lower than that of IAI counterparts with the same thickness of Ag layer. This must be a result of the better spreadability of Ag on AZO underlayer.

From the curves shown in the figure, it can be found that the transmittance values at wavelength of 1000 nm for the ZAZ are lower than those for IAI counterparts with the same thickness of Ag layer. However, the comparison between Figures 5(b) and 5(f) is an exception since the peak of curve in Figure 5(f) is widened due to the optical matching of three layers. According to Drude theory [32], the reflectivity in infrared region of conductive films is related to their electrical properties, and high reflectivity corresponds to low electrical resistivity. With the light wavelength increasing from visible region to infrared region, the transmittance of a conductive film decreases sharply and the big descent slope of its curve corresponds to low electrical resistivity [33]. From this point, the lower transmittance value at wavelength of 1000 nm means the lower electrical resistivity. Therefore, from the transmittance values at wavelength of 1000 nm it can also be showed that the sheet resistance of the ZAZ is lower than that of IAI counterparts with the same thickness of Ag layer.

Compared with the sheet resistance of bilayer shown in Table 1, the sheet resistances of the sandwiched layers shown by annotations in Figure 5 are slightly larger, especially for those of IAI. For example, the sheet resistances of IAI with 11 nm Ag layer are bigger than those of the ITO/Ag bilayer with 10 nm Ag layer, and some of the ZAZ with 9 nm Ag layer exhibit bigger sheet resistances than that of the AZO/Ag bilayer with 8 nm Ag layer. It may result from the damage of Ag layer caused from the bombardment during the subsequent deposition of ITO or AZO upperlayer. Since the connections between islands of Ag on the ITO are poorer than those on AZO, the effect of the bombardment on the sheet resistance deterioration of the IAI sandwiched layer is larger.

Beside the sheet resistance, the transmittance, another important property of a transparent conductive film, is also affected by Ag layer thickness. With increasing its thickness, the light transmittance decreases significantly. Therefore, transparent conductive oxide (TCO) layers are used for purpose of optical matching to improve the transmittance. As shown in Figure 5, the thickness of ITO or AZO has a great influence on the position and value of the light transmittance peak due to the optical interference effect. For every group of IAI and ZAZ sandwiched layers with the same thickness of

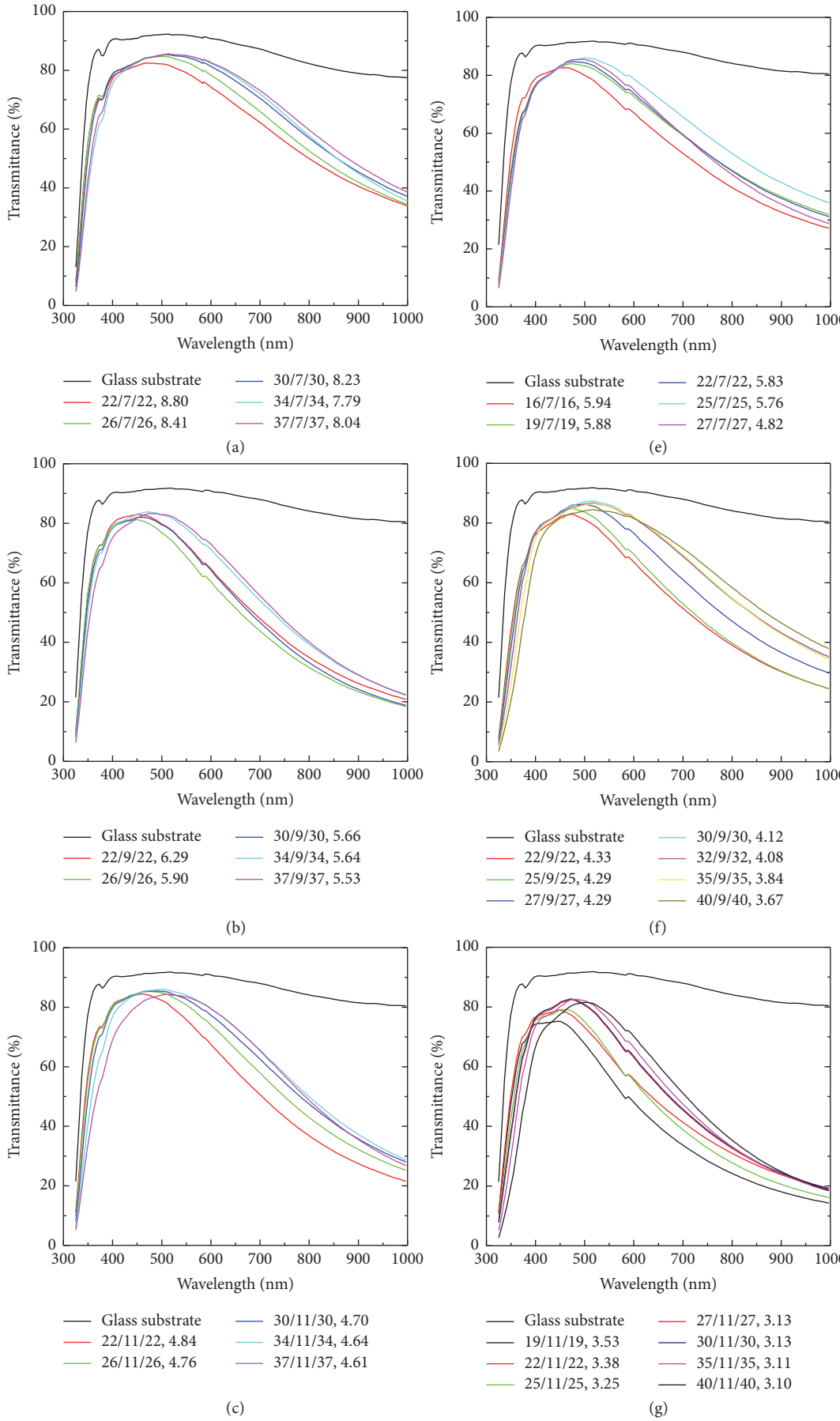

Figure 5: Continued.

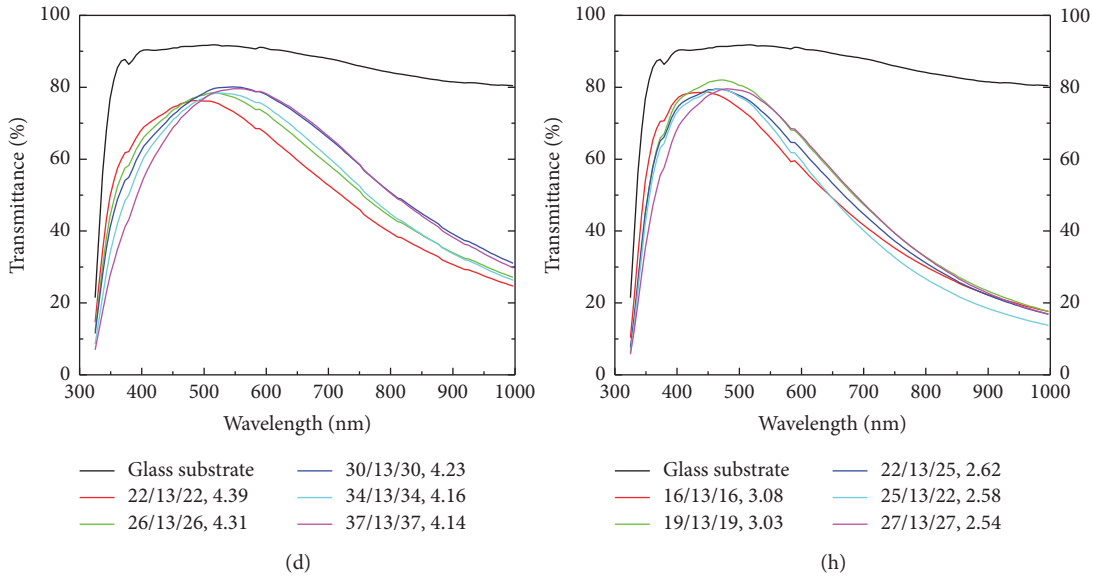

Figure 5: Performance of IAI (a–d) and ZAZ (e–h) with different layer thicknesses.

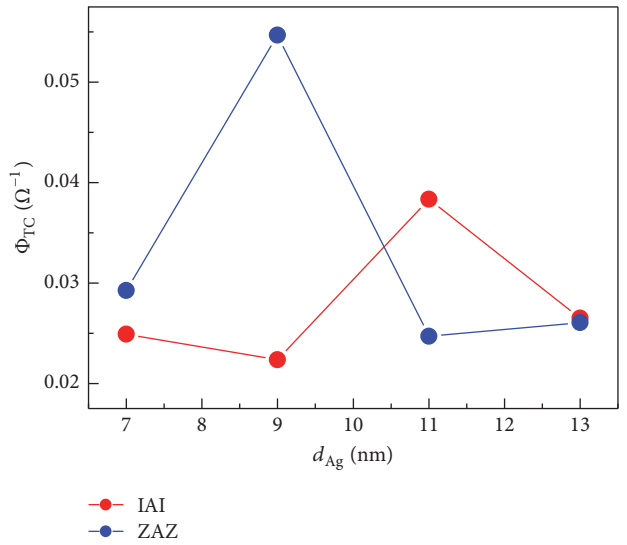

Figure 6: IAI and ZAZ Haacke figure of merit.

Table 2: Haacke figure of merit of IAI and ZAZ sandwiched layers.

Sandwiched layers	T_{550}, %	R_S, Ω/sq	Φ_{TC}, Ω^{-1}
ITO (34 nm)/Ag (7 nm)/ITO (34 nm)	84.87	7.79	0.02488
ITO (37 nm)/Ag (7 nm)/ITO (37 nm)	85.14	8.04	0.02489
ITO (34 nm)/Ag (9 nm)/ITO (34 nm)	78.64	5.64	0.01604
ITO (37 nm)/Ag (9 nm)/ITO (37 nm)	79.73	5.53	0.02237
ITO (34 nm)/Ag (11 nm)/ITO (34 nm)	84.14	4.64	0.03833
ITO (37 nm)/Ag (11 nm)/ITO (37 nm)	83.52	4.61	0.03583
ITO (30 nm)/Ag (13 nm)/ITO (30 nm)	80.21	4.23	0.02606
ITO (37 nm)/Ag (13 nm)/ITO (37 nm)	79.59	4.14	0.02464
AZO (25 nm)/Ag (7 nm)/AZO (25 nm)	83.69	5.76	0.02926
AZO (27 nm)/Ag (7 nm)/AZO (27 nm)	81.39	4.82	0.02646
AZO (32 nm)/Ag (9 nm)/AZO (32 nm)	85.81	4.08	0.05305
AZO (35 nm)/Ag (9 nm)/AZO (35 nm)	85.55	3.84	0.05469
AZO (40 nm)/Ag (9 nm)/AZO (40 nm)	83.88	3.67	0.04698
AZO (35 nm)/Ag (11 nm)/AZO (35 nm)	75.15	3.11	0.01847
AZO (40 nm)/Ag (11 nm)/AZO (40 nm)	77.34	3.10	0.02470
AZO (19 nm)/Ag (13 nm)/AZO (19 nm)	74.45	3.03	0.01727
AZO (27 nm)/Ag (13 nm)/AZO (27 nm)	74.49	2.54	0.02071

Ag layer, with increasing the thickness of ITO or AZO, the peak shifts to right and peak transmittance value increases at first and then decreases.

According to the performances of the samples shown in Figure 5, some samples with better performances are selected and their Haacke figure of merit Φ_{TC} is calculated and listed in Table 2. From samples with the same thickness of Ag layer, the ones with the biggest Φ_{TC} are picked out to form a relation between Φ_{TC} and thickness of Ag layer, as shown in Figure 6. The maximum Φ_{TC} (0.03833 Ω^{-1}) of IAI corresponds to the thickness of 11 nm, while that (0.05469 Ω^{-1}) of ZAZ corresponds to the thickness of 9 nm. Moreover, Φ_{TC} of the latter is much higher than that of the former. This may benefit from the better spreadability of Ag layer on AZO layer, which prompts the formation of uniform and continuous Ag layer in a much thinner thickness. The thickness match of ZAZ corresponding to the maximum Φ_{TC} is 35 nm/9 nm/35 nm with a light transmittance of 85.55% at 550 nm and a sheet resistance of 3.84 Ω/sq.

4. Conclusions

Single layers of indium tin oxide (ITO), aluminum-doped zinc oxide (AZO), and Ag, bilayers of ITO/Ag and AZO/Ag, and sandwiched layers of ITO/Ag/ITO (IAI) and AZO/Ag/AZO (ZAZ) were fabricated on ordinary glass substrates using magnetron sputtering. Compared with those on

glass substrate and ITO, the Ag has a better spreadability and the Ag layer is deposited more uniformly and continuously on AZO. In addition, the sheet resistances of the sandwiched layers are slightly larger than those of bilayers, which may result from the damage of Ag layer caused from the bombardment during the subsequent deposition of ITO or AZO upperlayer. With the matching of AZO (35 nm)/Ag (9 nm)/AZO (35 nm) (ZAZ), the transmittance, sheet resistance, and Haacke figure of ZAZ multilayer are 85.55%, 3.84 Ω/sq, and 0.05469 Ω^{-1}, respectively, showing a high performance.

Conflicts of Interest

The authors declare that they have no conflicts of interest.

Acknowledgments

This work was supported by Jinan government financial support (JK201303067 and 201305033), Shandong government financial support (L37002013098), NSFC (51471099), and China 973 project (no. 2012CB825702). The authors are grateful to Professor Tongguang Zhai from University of Kentucky for his valuable discussions and assistance in the present paper.

References

[1] C. Guillén and J. Herrero, "TCO/metal/TCO structures for energy and flexible electronics," *Thin Solid Films*, vol. 520, no. 1, pp. 1–17, 2011.

[2] C. Guillén and J. Herrero, "ITO/metal/ITO multilayer structures based on Ag and Cu metal films for high-performance transparent electrodes," *Solar Energy Materials and Solar Cells*, vol. 92, no. 8, pp. 938–941, 2008.

[3] C. H. Hong, Y. J. Jo, H. A. Kim, I.-H. Lee, and J. S. Kwak, "Effect of electron beam irradiation on the electrical and optical properties of ITO/Ag/ITO and IZO/Ag/IZO films," *Thin Solid Films*, vol. 519, no. 20, pp. 6829–6833, 2011.

[4] I. Crupi, S. Boscarino, V. Strano, S. Mirabella, F. Simone, and A. Terrasi, "Optimization of ZnO:Al/Ag/ZnO:Al structures for ultra-thin high-performance transparent conductive electrodes," *Thin Solid Films*, vol. 520, no. 13, pp. 4432–4435, 2012.

[5] F. Wang, M. Z. Wu, Y. Y. Wang, Y. M. Yu, X. M. Wu, and L. J. Zhuge, "Influence of thickness and annealing temperature on the electrical, optical and structural properties of AZO thin films," *Vacuum*, vol. 89, pp. 127–131, 2013.

[6] J. Ho Kim, Y.-J. Moon, S.-K. Kim, Y.-Z. Yoo, and T.-Y. Seong, "Al-doped ZnO/Ag/Al-doped ZnO multilayer films with a high figure of merit," *Ceramics International*, vol. 41, no. 10, pp. 14805–14810, 2015.

[7] S. Yu, W. Zhang, L. Li, D. Xu, H. Dong, and Y. Jin, "Optimization of SnO_2/Ag/SnO_2 tri-layer films as transparent composite electrode with high figure of merit," *Thin Solid Films*, vol. 552, pp. 150–154, 2014.

[8] S. H. Yu, L. X. Li, D. Xu, H. L. Dong, and Y. X. Jin, "Characterization of SnO_2/Cu/SnO_2 sandwiched layers for high performance transparent conducting electrodes," *Thin Solid Films*, vol. 562, pp. 501–505, 2014.

[9] L. Liu, S. Ma, H. Wu et al., "Effect of the annealing process on electrical and optical properties of SnO_2/Ag/SnO_2 nanometric multilayer film," *Materials Letters*, vol. 149, Article ID 18549, pp. 43–46, 2015.

[10] H. J. Park, J. H. Park, J. I. Choi, J. Y. Lee, J. H. Chae, and D. Kim, "Fabrication of transparent conductive films with a sandwich structure composed of ITO/Cu/ITO," *Vacuum*, vol. 83, no. 2, pp. 448–450, 2008.

[11] S. Song, T. Yang, M. Lv et al., "Effect of Cu layer thickness on the structural, optical and electrical properties of AZO/Cu/AZO tri-layer films," *Vacuum*, vol. 85, no. 1, pp. 39–44, 2010.

[12] D. Kim, "Low temperature deposition of transparent conducting ITO/Au/ITO films by reactive magnetron sputtering," *Applied Surface Science*, vol. 256, no. 6, pp. 1774–1777, 2010.

[13] T. Dimopoulos, G. Radnoczi, B. Pécz, and H. Brückl, "Characterization of ZnO:Al/Au/ZnO:Al trilayers for high performance transparent conducting electrodes," *Thin Solid Films*, vol. 519, no. 4, pp. 1470–1474, 2010.

[14] S. Boscarino, I. Crupi, S. Mirabella, F. Simone, and A. Terrasi, "TCO/Ag/TCO transparent electrodes for solar cells application," *Applied Physics A*, vol. 116, no. 3, pp. 1287–1291, 2014.

[15] A. Klöppel, W. Kriegseis, B. K. Meyer et al., "Dependence of the electrical and optical behaviour of ITO-silver-ITO multilayers on the silver properties," *Thin Solid Films*, vol. 365, no. 1, pp. 139–146, 2000.

[16] A. Indluru and T. L. Alford, "Effect of Ag thickness on electrical transport and optical properties of indium tin oxide-Ag-indium tin oxide multilayers," *Journal of Applied Physics*, vol. 105, no. 12, Article ID 123528, 2009.

[17] H.-W. Wu, R.-Y. Yang, C.-M. Hsiung, and C.-H. Chu, "Influence of Ag thickness of aluminum-doped ZnO/Ag/aluminum-doped ZnO thin films," *Thin Solid Films*, vol. 520, no. 24, pp. 7147–7152, 2012.

[18] J.-A. Jeong and H.-K. Kim, "Low resistance and highly transparent ITO-Ag-ITO multilayer electrode using surface plasmon resonance of Ag layer for bulk-heterojunction organic solar cells," *Solar Energy Materials and Solar Cells*, vol. 93, no. 10, pp. 1801–1809, 2009.

[19] R. Alvarez, J. C. González, J. P. Espinós, A. R. González-Elipe, A. Cueva, and F. Villuendas, "Growth of silver on ZnO and SnO_2 thin films intended for low emissivity applications," *Applied Surface Science*, vol. 268, pp. 507–515, 2013.

[20] G. Zhao, W. Wang, T.-S. Bae et al., "Stable ultrathin partially oxidized copper film electrode for highly efficient flexible solar cells," *Nature Communications*, vol. 6, pp. 8830–8837, 2015.

[21] J. H. Kim, T.-W. Kang, S.-I. Na, Y.-Z. Yoo, and T.-Y. Seong, "ITO-free inverted organic solar cells fabricated with transparent and low resistance ZnO/Ag/ZnO multilayer electrode," *Current Applied Physics*, vol. 15, no. 7, pp. 829–832, 2015.

[22] C. J. Lee, H. K. Lin, S. Y. Sun, and J. C. Huang, "Characteristic difference between ITO/ZrCu and ITO/Ag bi-layer films as transparent electrodes deposited on PET substrate," *Applied Surface Science*, vol. 257, no. 1, pp. 239–243, 2010.

[23] J.-H. Lee, S.-H. Lee, K.-L. Yoo, N.-Y. Kim, and C. K. Hwangbo, "Deposition of multi-period low-emissivity filters for display application by RF magnetron sputtering," *Surface and Coatings Technology*, vol. 158-159, pp. 477–481, 2002.

[24] K. S. Gadre and T. L. Alford, "Contact angle measurements for adhesion energy evaluation of silver and copper films on parylene-n and SiO_2 substrates," *Journal of Applied Physics*, vol. 93, no. 2, pp. 919–923, 2003.

[25] J. Lv, "Effect of wettability on surface morphologies and optical properties of Ag thin films grown on glass and polymer

substrates by thermal evaporation," *Applied Surface Science*, vol. 273, pp. 215–219, 2013.

[26] Y.-S. Park, H.-K. Park, J.-A. Jeong et al., "Comparative investigation of transparent ITO/Ag/ITO and ITO/Cu/ITO electrodes grown by dual-target DC sputtering for organic photovoltaics," *Journal of the Electrochemical Society*, vol. 156, no. 7, pp. H588–H594, 2009.

[27] Y. Tsuda, H. Omoto, K. Tanaka, and H. Ohsaki, "The underlayer effects on the electrical resistivity of Ag thin film," *Thin Solid Films*, vol. 502, no. 1-2, pp. 223–227, 2006.

[28] Y.-S. Lin and Z.-S. Wu, "Leading nano-Ag particles on the textured seed layer to enhance the optoelectronic properties of Al-doped ZnO layers," *Vacuum*, vol. 116, pp. 139–143, 2015.

[29] G. Haacke, "New figure of merit for transparent conductors," *Journal of Applied Physics*, vol. 47, no. 9, pp. 4086–4089, 1976.

[30] A. El Hajj, B. Lucas, M. Chakaroun, R. Antony, B. Ratier, and M. Aldissi, "Optimization of ZnO/Ag/ZnO multilayer electrodes obtained by Ion Beam Sputtering for optoelectronic devices," *Thin Solid Films*, vol. 520, no. 14, pp. 4666–4668, 2012.

[31] M. Ohring, *Materials Science of Thin Films: Deposition and Structure*, Academic Press, San Diego, Calif, USA, 2002.

[32] G. Frank, E. Kauer, and H. Köstlin, "Transparent heat-reflecting coatings based on highly doped semiconductors," *Thin Solid Films*, vol. 77, no. 1–3, pp. 107–118, 1981.

[33] C. Schaefer, G. Bräuer, and J. Szczyrbowski, "Low emissivity coatings on architectural glass," *Surface and Coatings Technology*, vol. 93, no. 1, pp. 37–45, 1997.